

## Nanolaser on carbon nanotube

© I.V. Dzedolik, A.A. Kuzmin, V.E. Polyakov

V.I. Vernadsky Crimean Federal University, Physics and Technology Institute, Simferopol, Russia

e-mail: igor.dzedolik@cfuv.ru

Received November 01, 2025

Revised December 04, 2025

Accepted December 05, 2025

The theoretical model of the nanolaser on carbon nanotube with zigzag chirality, which has semiconductor properties, is considered. Periodic surface inhomogeneities forming Bragg gratings are realized at the ends of the nanotube, i.e. such nanotube is a nanoresonator. It is shown that at pumping the nanoresonator by optical radiation, the coherent flow of surface plasmon-polaritons occurs in the nanolaser when the generation threshold is exceeded.

**Keywords:** carbon nanotube, nanoresonator, nanolaser, plasmon-polariton.

DOI: 10.61011/EOS.2026.01.63221.8732-25

### Introduction

In today's world the trends for miniaturization of optical and telecommunication systems dictate the need for design and development of appropriate devices [1–4]. In recent years, great advances in the production of optical micro- and nanostructures have significantly reduced the size of many optical components. Reducing the devices geometry not only helps to lower the energy consumption, but also contributes to a higher density of nanodevices on photonic chips, which is crucial for the high-tech systems where small sizes and efficiency are a must.

In this regard, plasmonic circuit technology is promising for use in various fields, such as nanoelectronics, optoelectronics, nanophotonics, and fiber-optic communications. The elements of the circuitry engineering include the nanoscale waveguides and nano-resonators [4], as well as plasmon logic elements [5–7]. In addition, the implementation of plasmonic circuitry requires the presence of nanoscale radiation sources — plasmonic signal generators — nanolasers [3,8–10].

Special attention should be paid to the concept of a nanolaser with minimal geometry, proposed to enhance and generate a coherent near field [11,12]. A spaser is a nanoscale device consisting of a metal nanoparticle supporting plasmonic excitations and an amplifying medium with an inverse population. The amplifying medium is excited by external pumping, which, in its turn, excites localized plasmonic modes in the metal nanoparticle. Spasers have been deployed and used in nanophotonics to create ultra-compact coherent light sources [13,14], however, the degree of coherence of the spaser radiation is low.

Currently, a large number of different nanolasers have been developed and deployed, including nanolasers based on graphene [15–17], quantum wells [18], semiconductor nanowires [19–22], and high-index dielectric nanostructures used for non-plasmonic nanolasers [23]. Terahertz generators based on the carbon nanotubes (CNT) are outlined in paper [24].

Since instead of a photon flow a plasmon flow is generated in the nanolaser, it makes it possible to overcome the diffraction limit as a result of exponential decay of the surface plasmon field, i.e., to provide a nanometer coherent radiation source. Nanolasers are capable of generating a coherent electromagnetic radiation, including optical radiation at sub-wavelengths, which makes them the first choice devices in the new generation computing systems and sensors.

Like any other laser, a nanolaser consists of three key elements: a resonator, an amplifying medium, and an external energy source (pumping source). In nanolasers, the developed resonators shall provide a sub-wavelength size of the optical beam or plasmon flow and have sufficient Q-factor, which is necessary to generate coherent radiation at reasonable pumping levels [4]. High quality factor makes it possible to reduce pumping thresholds, which is critical for the efficient operation of nanolasers in miniature devices. The higher the Q-factor of the resonator and the efficiency of pumping-amplifying medium interaction, the lower the required pumping threshold, which makes such systems more economical and efficient.

CNT are single-layer or multilayer tubular structures consisting of carbon atoms orderly arranged on a nanotube surface in the form of hexagons, as well as pentagons and heptagons in the region of the nanotube bend [25–28]. CNT have both semiconductor and metallic properties, depending on the type of lattice and the chirality of CNT. When propagating ultrashort pulses of the optical range, CNT exhibit nonlinear properties [29,30]. Moreover, the shape of ultrashort laser pulses affects the probability of atoms excitation of [31,32] in CNT. The modern element base of plasmonic circuitry is designed to operate at telecommunication frequencies [4].

In this study, a model of a CNT nanolaser operating at a telecommunication frequency is proposed and investigated in theory. In the nanolaser, it is proposed to use CNT with chirality of a „zigzag“ type featuring semiconductor

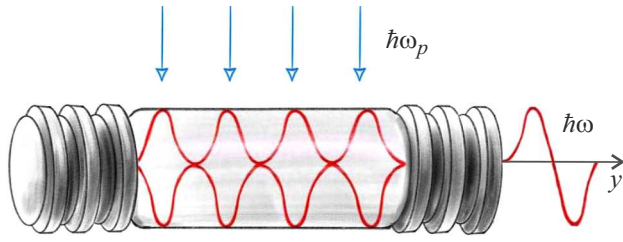


Figure 1. CNT nanolaser.

properties. Periodic surface irregularities forming Bragg gratings should be realized at the nanotube ends, i.e., such a nanotube is a resonator itself. It is possible to fabricate a nano-resonator with Bragg gratings using CNT cultivation technologies while varying their growth modes [33].

When the nanolaser resonator on a CNT is pumped with optical radiation, a coherent stream of plasmon polaritons at a telecommunication frequency occurs in it when the generation threshold is exceeded, which is determined by the length of the resonator. A flow of coherent plasmon polaritons from the nanolaser resonator to the CNT can be directed into a plasmon waveguide, including a CNT-based waveguide connected to the resonator mirror. Coherent plasmon flow can be used in plasmon logic gates. In addition, the CNT nanolaser can be used as a signal amplifier in plasmon circuitry.

## Nanolaser model

Let's consider the suggested model of a CNT nanolaser. The amplifying medium (working fluid) and resonator for the nanolaser is a „zigzag“ CNT with semiconductor properties, at the ends of which there are periodic surface inhomogeneities like Bragg gratings, and the nanolaser is pumped by radiation in the optical range (Fig. 1).

## CNT plasmon modes

An electromagnetic wave with a frequency of  $\omega$  interacts with conductivity electrons and bound electrons in the nanotube, generating surface plasmon polaritons in CNT. For a thin nanotube with a radius of  $r_0$ , if its thickness is much less than the mode wavelength,  $r_0 \ll \lambda = 2\pi/\beta$ , the solutions of Maxwell's equations make physical sense for the components of the electromagnetic field, which tend to zero with the growing distance  $r \rightarrow \infty$  from the nanotube axis.

Expressions for the components of plasmon-polariton monochromatic ( $\sim \exp(-i\omega t)$ ) surface wave propagating along the CNT can be obtained from the Maxwell system of equations for a non-magnetic medium ( $\mu = 1$ ) with a dielectric constant of  $\varepsilon$ . Maxwell vector equations for the field components  $\nabla \times \mathbf{H} = -ik_0\varepsilon\mathbf{E}$  and  $\nabla \times \mathbf{E} = ik_0\mathbf{H}$ , where  $k_0 = \omega/c$ , in cylindrical coordinate system  $(r, \varphi, z)$

have their solutions beyond the nanotube as Macdonald functions [7]:

$$\begin{aligned} E_r &= \frac{r_0^2}{w^2} \left[ A \frac{-i\beta w}{r_0 K_l(w)} K_l\left(\frac{wr}{r_0}\right) + B \frac{k_0}{K_l(w)} \frac{l}{r} K_l\left(\frac{wr}{r_0}\right) \right], \\ E_\varphi &= \frac{r_0^2}{w^2} \left[ A \frac{\beta}{K_l(w)} \frac{l}{r} K_l\left(\frac{wr}{r_0}\right) + B \frac{ik_0 w}{r_0 K_l(w)} K_l'\left(\frac{wr}{r_0}\right) \right], \\ H_r &= \frac{r_0^2}{w^2} \left[ B \frac{-i\beta w}{r_0 K_l(w)} K_l'\left(\frac{wr}{r_0}\right) - A \frac{k_0 \varepsilon}{K_l(w)} \frac{l}{r} K_l\left(\frac{wr}{r_0}\right) \right], \\ H_\varphi &= \frac{r_0^2}{w^2} \left[ B \frac{\beta}{K_l(w)} \frac{l}{r} K_l\left(\frac{wr}{r_0}\right) - A \frac{ik_0 \varepsilon w}{r_0 K_l(w)} K_l'\left(\frac{wr}{r_0}\right) \right], \\ E_z &= A \frac{K_l(wr/r_0)}{K_l(w)}, \quad H_z = B \frac{K_l(wr/r_0)}{K_l(w)}, \end{aligned} \quad (1)$$

where the prime denotes the derivative of the function with respect to its argument,  $w^2 = r_0^2(\beta^2 - k_0^2\varepsilon)$ . The modes versus time, versus azimuthal and longitudinal coordinate are expressed as

$$E_j, H_j \sim \exp(-i\omega t + il\varphi + i\beta z), \quad l = 0, \pm 1, \pm 2, \dots,$$

$\varepsilon$  — dielectric permittivity of the medium around the CNT. The components of modes with zero azimuth index  $l = 0$  are found from the expressions (1) taking into account the property of Macdonald function  $K_0' = -K_1$ :

TM-mode

$$\begin{aligned} E_r &= i \frac{\beta_0 r_0}{w} A \frac{K_1(wr/r_0)}{K_0(w)}, \quad H_\varphi = i \frac{\varepsilon k_0 r_0}{w} A \frac{K_1(wr/r_0)}{K_0(w)}, \\ E_z &= A \frac{K_0(wr/r_0)}{K_0(w)}, \end{aligned} \quad (2)$$

TE-mode

$$\begin{aligned} H_r &= i \frac{\beta_0 r_0}{w} B \frac{K_1(wr/r_0)}{K_0(w)}, \quad E_\varphi = -i \frac{k_0 r_0}{w} B \frac{K_1(wr/r_0)}{K_0(w)}, \\ H_z &= B \frac{K_0(wr/r_0)}{K_0(w)}, \end{aligned} \quad (3)$$

where  $\beta_0$  — propagation constant of the corresponding mode.

## Modal dispersion equation

To determine the propagation constants of  $\beta(\omega)$  plasmon-polariton modes in CNT, it is necessary to obtain a dispersion equation. We use Leontovich boundary conditions  $E_z = \xi H_\varphi$  and  $H_z = E_\varphi/\xi$  on the nanotube surface at  $r = r_0$ , where  $\xi = \sqrt{\mu_c/\varepsilon_c}$  — surface impedance of a conductive surface [34]. Given that for CNT  $\mu_c = 1$ , i.e. impedance is equal  $\xi = 1/\sqrt{\varepsilon_c}$ , from the system of equations (1) we get the dispersion equation for the

propagation constants  $\beta_l(\omega)$  of plasmon polariton CNT modes (see Appendix A)

$$K_l^2(w) + \varepsilon \frac{k_0^2 r_0^2}{w^2} K_l'^2(w) + i \frac{\varepsilon - \varepsilon_c}{\sqrt{\varepsilon_c}} \times \frac{k_0 r_0}{w} K_l(w) K_l'(w) = l^2 \frac{\beta^2 r_0^2}{w^4} K_l^2(w). \quad (4)$$

Macdonald function argument  $w = r_0(\beta^2 - k_0^2 \varepsilon)^{1/2}$  shall have a valid value, i.e.  $\beta > k_0 \sqrt{\varepsilon}$ , permittivity of the environment  $\varepsilon$  — real value.

For the modes with azimuthal index  $l = 0$  from the equation (4) we get a dispersion equation as

$$K_0^2(w) + \varepsilon \frac{k_0^2 r_0^2}{w^2} K_1^2(w) - i \frac{\varepsilon - \varepsilon_c}{\sqrt{\varepsilon_c}} \frac{k_0 r_0}{w} K_0(w) K_1(w) = 0. \quad (5)$$

On the surface of the nanotube ( $r = r_0$ ), modes with zero azimuthal index  $l = 0$  transform into planar waves. This follows from the substitution into expressions for modes (2) and (3) of the relation  $K_1(w)/K_0(w)$  — obtained from the dispersion equation (5) (Appendix A), where it is required to take  $\frac{K_1(w)}{K_0(w)} = -i \frac{w \sqrt{\varepsilon_c}}{\varepsilon k_0 r_0}$  for TM-mode and  $\frac{K_1(w)}{K_0(w)} = i \frac{w}{\sqrt{\varepsilon_c} k_0 r_0}$  — for TE-mode. The amplitudes of the mode components with zero azimuth index — are expressed as:

TM-mode —

$$E_r = \frac{\beta_0 \sqrt{\varepsilon_c}}{\varepsilon k_0} A, \quad H_\varphi = \sqrt{\varepsilon_c} A, \quad E_z = A, \quad (6)$$

TE-mode —

$$H_r = -\frac{\beta_0}{\sqrt{\varepsilon_c} k_0} B, \quad E_\varphi = \frac{1}{\sqrt{\varepsilon_c}} B, \quad H_z = B. \quad (7)$$

The modes propagation constants are determined from the ratio  $K_1/K_0$ , given that

$$\sqrt{\varepsilon_c} = (\varepsilon_c'^2 + \varepsilon_c''^2)^{1/4} \exp(i\delta) = \sqrt{|\varepsilon_c|} (\cos \delta + i \sin \delta),$$

where  $\delta = \arctan(\varepsilon_c''/\varepsilon_c')$ ,  $\varepsilon_c'$  and  $\varepsilon_c''$  — are the real and imaginary parts of CNT dielectric permittivity. Then, we obtain the dispersion equations for the TM-mode

$$w K_0(w) - \varepsilon_{\text{TM}} K_1(w) = 0, \quad (8)$$

for TE-mode

$$w K_0(w) - \varepsilon_{\text{TE}} K_1(w) = 0, \quad (9)$$

where  $\varepsilon_{\text{TM}} = \frac{\varepsilon k_0 r_0}{\sqrt{|\varepsilon_c|}}$ ,  $\varepsilon_{\text{TE}} = \sqrt{|\varepsilon_c|} k_0 r_0$ . In equations (8) and (9) it is taken into account that the imaginary part of the equations is zero ( $i \varepsilon_{\text{TM,TE}} \cos(\delta) = 0$ ), while the real part, i.e.  $\varepsilon_{\text{TE}} = \sqrt{|\varepsilon_c|} k_0 r_0 \delta = \pi/2$  and  $\sin(\delta) = 1$ . The volume  $V$  of the mode field is estimated taking into account the expression for MacDonald functions:

$$K_n \approx \sqrt{\pi r_0 / 2 w r} \exp(-w r / r_0),$$

assuming that  $r = (\beta^2 - k_0^2 \varepsilon)^{-1/2}$ ; then  $V = \pi(r^2 - r_0^2)L$ , where  $L$  — resonator length.

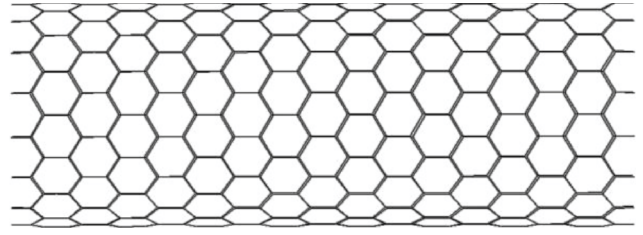


**Figure 2.** CNT of „zigzag“ type with the chirality indices (17,0); distance between adjacent carbon atoms  $d_0 = 0.142$  nm.

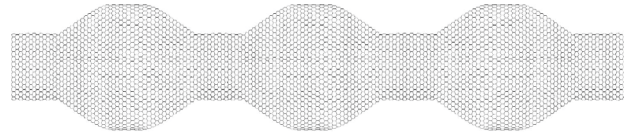


**Figure 3.** Bragg grating — periodic surface inhomogeneities at the CNT ends with chirality indices (13,0)–(17,0).

## Resonator of CNT nanolaser

The nanolaser resonator (Fig. 1) is a CNT with a „zigzag“ type chirality (Fig. 2) with periodic boundary inhomogeneities at the ends of the nanotube — Bragg gratings as mirrors. Bragg gratings are implemented by periodically changing the diameter of CNT without compromising its chirality (Fig. 3).

Consider the propagation of modes with an azimuthal index  $l = 0$  over the CNT surface (expressions (6) and (7)). Plasmon polariton mode with the propagation constant  $\beta_0$ , which is defined by the environment dielectric constants  $\varepsilon$  and CNT  $\varepsilon_c$ , as well as by radius of the nanotube  $r_0$ , falls onto the boundary inhomogeneity — the Bragg grating. For maximum reflection from the Bragg grating, there shall be constructive interference of waves  $2n_{\text{ef}}d = \lambda/2$  when reflected from a layer with a refractive index of  $n_{\text{ef}}$  and a thickness of  $d$ , i.e., the layer thickness shall be  $d = \lambda/4n$ . In CNT, for modes in the boundary inhomogeneity, we have  $2\beta_h d = \pi$ , i.e., the length of the inhomogeneity should be  $d = \lambda_h/4$ . When plasmon-polariton waves are reflected from the nano-resonator mirrors, conditions exist for the occurrence of a standing wave, i.e., multiple stimulated emission of surface plasmons into the CNT, which leads to the generation of a coherent plasmon-polariton flux, which is discharged from the nanolaser into a plasmon waveguide. The inhomogeneities of the CNT boundary represent periodic changes in the radius of the nanotube, i.e., the Bragg grating (Fig. 3), which is characterized by the matrix (Appendix B)

$$M = \begin{pmatrix} m_{11} & m_{12} \\ m_{21} & m_{22} \end{pmatrix}. \quad (10)$$

The amplitude reflection coefficients  $\rho$  are expressed as:

for TM mode

$$\rho = \frac{E_{rr}}{E_{ri}} = \frac{m_{11} + m_{12} \frac{\epsilon k_0}{\beta_0} - \frac{\beta_0}{\epsilon k_0} m_{21} - m_{22}}{m_{11} + m_{12} \frac{\epsilon k_0}{\beta_0} + \frac{\beta_0}{\epsilon k_0} m_{21} + m_{22}}, \quad (11)$$

for TE-mode

$$\rho = \frac{E_{\varphi r}}{E_{\varphi i}} = \frac{m_{22} - \frac{k_0}{\beta_0} m_{21} - m_{11} + \frac{\beta_0}{k_0} m_{12}}{m_{11} - \frac{\beta_0}{k_0} m_{12} - \frac{k_0}{\beta_0} m_{21} + m_{22}}, \quad (12)$$

## Coherent generation of nano-laser

To operate the nanolaser in the coherent generation mode, it is necessary that the radiation gain in one cycle (the passage of the flow back and forth between the mirrors) exceeds the losses in the resonator and laser radiation. The nanolaser cycle includes two consecutive reflections from mirrors with effective reflection coefficients  $R_1$  and  $R_2$ , which take into account all losses, including radiation losses. The decay of the flow is proportional to the product of the reflection coefficients  $R_1 R_2$  on a path  $2L$  long per cycle, where  $L$  is the length of the resonator. Higher electromagnetic flow in the nanolaser in one cycle is equal to [35–37]

$$I = I_0 R_1 R_2 e^{2\alpha L} = I_0 \exp[2\alpha L - \ln(R_1 R_2)].$$

The generation occurs at  $2\alpha L > |\ln(R_1 R_2)|$ , i.e. the nanolaser generation threshold is equal

$$\alpha_0 = \frac{|\ln(R_1 R_2)|}{2L}. \quad (13)$$

Let's define Q-factor of the nanolaser resonator as  $Q = E/\delta E$ , where  $E = w_r S_r L$  — energy stored in the resonator,  $w_r$  — energy density of the forward and backward flows,  $S_r$  — resonator's cross-section area,  $\Delta E$  — energy losses per cycle. Energy losses per cycle may be found as

$$\Delta E = \frac{1}{2} w_r S_r L [1 - \exp(-\ln(R_1 R_2))].$$

The time of one cycle is  $t = 2L/v$ , where  $v$  — wave velocity, and period  $T_r = 2\pi/\omega$ , then, the energy losses per one oscillation make

$$\begin{aligned} \delta \tilde{E} &= \frac{\Delta E}{2L/v} T_r = \frac{w_r S_r L v T_r}{4L} \left( 1 - \frac{1}{\exp(\ln(R_1 R_2))} \right) \\ &\approx \frac{1}{4} w_r v S_r T_r |\ln(R_1 R_2)|. \end{aligned}$$

From here we find the Q-factor of the CNT nanoresonator

$$Q = \frac{N_{\lambda/2}}{|\ln(R_1 R_2)|},$$

where  $N_{\lambda/2} = 2L/(\lambda/2)$  — number of half-waves of the standing wave in the nano-resonator,  $\lambda = v T_r$  — wavelength. Expressing the generation threshold in terms of

the nanoresonator Q-factor, we obtain  $\alpha_0 = N_{\lambda/2}/Q2L$  or  $\alpha_0 \lambda/2 = Q^{-1}$ .

The length of the nanoresonator is determined by the number of half-waves of excited modes:  $L = (\lambda/2)n = (\pi/\beta)n$ , where  $n = 1, 2, \dots$ , and minimum length of the nanoresonator is found taking into account the gain factor  $\alpha \geq \alpha_0$  at  $\alpha \lambda/2 \geq Q^{-1}$  as  $L_{\min} = 1/\alpha Q$ .

## CNT electronic spectrum

To generate a plasmon-polariton flow, CNT shall exhibit semiconductor properties. The band structure of CNT is found from the dispersion equation [28]

$$\Delta E = \pm \gamma_{AB} \left\{ 1 + 4 \cos \frac{k_y a}{2} \left[ \cos \frac{\sqrt{3} k_x a}{2} + \cos \frac{k_y a}{2} \right] \right\}^{1/2}, \quad (14)$$

where  $\gamma_{AB}$  — overlapping integral for the nearest graphene lattice atoms. The quantization condition of the electron wave vector in the CNT is represented as

$$\mathbf{Rk} = (m\mathbf{r}_1 + n\mathbf{r}_2)(\mathbf{1}_x k_x + \mathbf{1}_y k_y) = 2\pi s, \quad (15)$$

where  $\mathbf{R} = m\mathbf{r}_1 + n\mathbf{r}_2$ ,  $\mathbf{k} = \mathbf{1}_x k_x + \mathbf{1}_y k_y$  — electron wave vector,  $\mathbf{r}_1$  and  $\mathbf{r}_2$  — basis vectors of graphene unit cell,  $r_1 = r_2 = a$  — graphene lattice parameter,  $(m, n)$  — CNT chirality indices,  $s = 1, 2, 3, \dots$  — an integer numbering the allowed states of the electron.

In the individual case the CNT may have a „zigzag“ structure  $(m, 0)$ , for which  $k_y = \frac{2\pi}{\sqrt{3}d_0 m}$ ,  $s = 1, 2, 3, \dots, m$ , hence, we obtain the expressions for the CNT band gap FWHM.

$$\Delta E = \gamma_{AB} \left( 1 + 4 \cos \frac{\pi s}{m} \cos \frac{3k_x d_0}{2} + 4 \cos^2 \frac{\pi s}{m} \right)^{1/2}. \quad (16)$$

The width of the band gap  $E_g = 2\Delta E$  in „zigzag“ CNT with semiconductor properties with indexes  $(m, 0)$  and diameter  $D = \frac{\sqrt{3}d_0}{\pi} m$ , where  $d_0 = 0.142$  nm — the distance between neighboring carbon atoms in the graphite plane, is found using expression (16). At that, the index  $m$  of „zigzag“ CNT shall not be a multiple of three, then FWHM of the band gap is not zero,  $\Delta E \neq 0$  [26,28].

Suppose that  $k_x$  vector changes in the first Brillouin zone:  $k_x = (-\frac{\pi}{T}, \frac{\pi}{T})$ , where  $T = a \sqrt{t_1^2 + t_2^2}$  — translation module vector  $\mathbf{T} = t_1 \mathbf{r}_1 + t_2 \mathbf{r}_2$  (perpendicular to vector  $\mathbf{R}$ ),  $t_1 = \frac{2n+m}{d}$ ,  $t_2 = -\frac{2m+n}{d}$ ,  $d$  — the largest common divider for  $2n+m$  and  $2m+n$ ,  $a = \sqrt{3}d_0$  [28]. Electronic spectra of „zigzag“ CNT with chirality indices (17.0) is given in Fig. 4. Analyzing the graphs in Fig. 4 we see that the band gap in „zigzag“ CNT with indices (17.0) is defined by the difference of energy in valence band and conductivity band  $E_g$  of the eleventh sub-band  $s_{11}$ .

## Inter-band electronic transitions

If an electron in the CNT with semiconductor properties interacts with the electromagnetic pumping field, then the

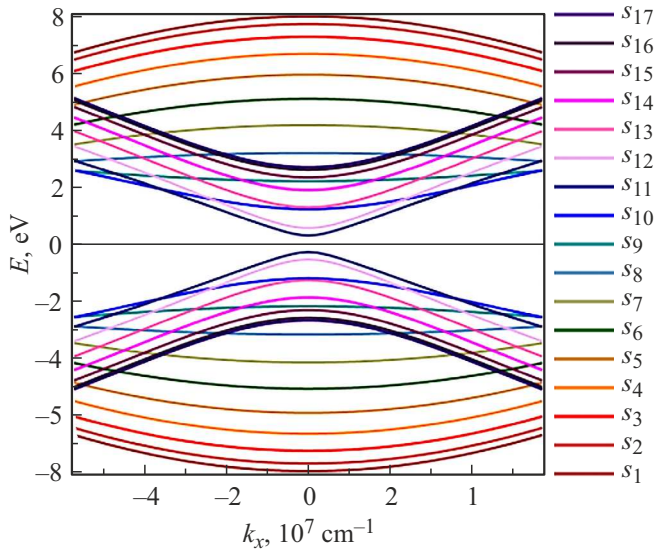


**Figure 4.** Electronic spectra of „zigzag“ CNT with chirality indices (17,0); number of subbands  $s = 1, \dots, 17$ .

probability of the electron transition to the state of  $n'$  from the state of  $n$  per unit time is

$$w_{nn'} = \frac{2\pi}{\hbar} |\hat{H}'_{nn'}|^2 \delta(E_n - E_{n'} - \hbar\omega)$$

(„golden rule“ of Fermi) [37]. The disturbance Hamiltonian in the interaction of an electron with electromagnetic field is given as

$$\hat{H}' = \frac{e}{2} \mathbf{r} \mathbf{E}_a (e^{i\omega t - i\mathbf{k}_{\text{opt}} \mathbf{r}}) + \text{c.c.},$$

where  $\mathbf{E}_a = \text{const}$  — amplitude of electric field. In this case, the matrix element of the disturbance operator is written as

$$\hat{H}'_{vc} = \frac{e}{2} \int d^3 r \psi_{vk}^*(\mathbf{r}) (\mathbf{r} \mathbf{E}_a) \psi_{ck'}(\mathbf{r}) e^{i(\mathbf{k}' - \mathbf{k} - \mathbf{k}_{\text{opt}}) \mathbf{r}}.$$

The magnitude of this integral tends to zero due to the oscillating multiplier, except in the case of  $\mathbf{k}' - \mathbf{k} = \mathbf{k}_{\text{opt}}$ .

At absolute zero temperature  $T = 0$ , all states of the valence band ( $v$ ) of the semiconductor CNT are filled, and the conductivity band ( $c$ ) is empty. In parabolic approximation for the sub-bands of the valence band and the conductivity band (Fig. 4), under the condition of a forward inter-band transition ( $k' = k \equiv k_x$ ), the electron energy is equal to the bands energy difference plus the band gap energy [37]:

$$E_c - E_v = \frac{\hbar^2 k^2}{2} \left( \frac{1}{m_c} + \frac{1}{m_v} \right) + E_g.$$

The probability of an electron moving from the valence band to the conductivity band per unit time in this case is

$$w_{vc} = \frac{2\pi}{\hbar} |\hat{H}'_{vc}|^2 \delta\left(\frac{\hbar^2 k^2}{2m_{vc}} + E_g - \hbar\omega\right),$$

where  $m_{vc} = m_v m_c / (m_v + m_c)$  — is the reduced effective mass of the electron.

Number of electron transitions

$$N = \int_0^\infty dk w_{vc} \rho(k)$$

with densities of electron states

$$\rho(k) = 2 \frac{4\pi k^2}{8\pi^3} V = \frac{k^2 V}{\pi^2}$$

for a  $V$  volume body is equal [37]

$$N = \frac{2V}{\hbar\pi} \int_0^\infty dk k^2 |\hat{H}'_{vc}|^2 \delta\left(\frac{\hbar^2 k^2}{2m_{vc}} + E_g - \hbar\omega\right).$$

At  $\frac{\hbar^2 k^2}{2m_{vc}} + E_g = \hbar\omega$  the number of interband transitions in CNT is

$$N = \frac{V(2m_{vc})^{3/2}}{\hbar^4 \pi} |\hat{H}'_{vc}|^2 \sqrt{\hbar\omega - E_g}. \quad (17)$$

## CNT dielectric permittivity

The dielectric permittivity of CNT is represented as (Appendix C)

$$\varepsilon_c(\omega) = 1 + \frac{2m\omega_e^2}{\hbar} \sum_n |r_{n0}|^2 \frac{\omega_{n0} - i\Gamma_n/2}{(\omega_{n0} - i\Gamma_n/2)^2 - \omega^2}, \quad (18)$$

where  $\omega_e^2 = 4\pi e^2 N_e / m_{\text{ef}}$  — square of the electron plasma frequency,  $m_{\text{ef}}$  — effective mass of an electron,  $N_e$  — number of electrons per unit volume. We assume that plasmon-polariton modes (expressions (1)–(3)) are excited at the frequency of the forward electronic transition  $\omega = \omega_{nn'}$  in CNT. Then the dielectric permittivity of the CNT during photon emission (absorption) at the electronic transition frequency  $\omega$  is equal to

$$\varepsilon_c(\omega) = 1 + \frac{8\pi e^2 |r_{nn'}|^2 N_e}{\hbar} \left[ \frac{4\omega}{16\omega^2 + \Gamma^2} + \frac{i}{\Gamma} \left( 1 + \frac{\Gamma^2}{16\omega^2 + \Gamma^2} \right) \right]. \quad (19)$$

Let us estimate the coefficient in front of brackets in expression (19) when there's a forward transition of electron during recombination from the conductivity band to the valence band. Assuming for electron  $e^2 / r_{nn'} = \hbar\omega$ , we get

$$\frac{8\pi e^2 |r_{nn'}|^2 N_e}{\hbar} = \frac{8\pi e^6 N_e}{\hbar^3 \omega^2}.$$

The relaxation frequency for such an electronic transition is  $\Gamma = \frac{2e^6 \omega}{3\hbar^3 c^3}$  (Appendix C). By substituting the expression

for  $\Gamma$  into coefficient  $\frac{8\pi e^6 N_e}{\hbar^3 \omega^2} = \frac{12\pi c^3 N_e}{\omega^3} \Gamma$ , we get the expression for CNT dielectric permittivity at transition frequency  $\omega$  as

$$\varepsilon_c(\omega) = 1 + 12\pi c^3 N_e \left[ \frac{4\Gamma}{\omega^2(16\omega^2 + \Gamma^2)} + \frac{i}{\omega^3} \left( 1 + \frac{\Gamma^2}{16\omega^2 + \Gamma^2} \right) \right]. \quad (20)$$

## Absorption coefficient

The CNT absorption coefficient is defined as the ratio of the absorbed power per unit volume,  $P_a = N\hbar\omega/V$ , to the average power density of the incident electromagnetic radiation flux passing through a unit area:

$$\alpha(\omega) = \frac{N\hbar\omega}{|\bar{\mathbf{S}}|V}, \quad (21)$$

where  $|\bar{\mathbf{S}}| = \frac{c}{8\pi} \overline{|\mathbf{E} \times \mathbf{H}|}$  — the time-average Poynting vector (Appendix D). For CNT modes with zero azimuthal index  $l = 0$ , we find the absorption coefficients for TM and TE modes from expression (21) by substituting the number of interband transitions (17) into it,

$$\alpha_{\text{TM}}(\omega) = \frac{(2m_{vc})^{3/2}}{\hbar^3 \pi} \frac{|\hat{H}'_{vc}|^2}{(c/4\pi)S_{\text{TM}}A^2} \omega \sqrt{\hbar\omega - E_g}, \quad (22)$$

$$\alpha_{\text{TE}}(\omega) = \frac{(2m_{vc})^{3/2}}{\hbar^3 \pi} \frac{|\hat{H}'_{vc}|^2}{(c/4\pi)S_{\text{TE}}B^2} \omega \sqrt{\hbar\omega - E_g}, \quad (23)$$

where

$$S_{\text{TM}} = \sqrt{\beta_0^2/k_0^2 + \varepsilon}, \quad S_{\text{TE}} = |\varepsilon|^{-1} \sqrt{\beta_0^2/k_0^2 + \varepsilon},$$

$\beta_0$  — TM- or TE-mode propagation constant, respectively. Substituting squares of matrix elements into expressions (22) and (23) (Appendix D), we obtain the absorption coefficients for the TM and TE modes:

$$\alpha_{\text{TM}}(\omega) = \frac{e^2(2m_{vc})^{3/2}}{c\hbar^3 \sqrt{\beta_0^2/k_0^2 + \varepsilon}} |y_{vc}|^2 \omega \sqrt{\hbar\omega - E_g}, \quad (24)$$

$$\alpha_{\text{TE}}(\omega) = \frac{e^2(2m_{vc})^{3/2}}{c\hbar^3 \sqrt{\beta_0^2/k_0^2 + \varepsilon}} r_0^2 |\varphi_{vc}|^2 \omega \sqrt{\hbar\omega - E_g}. \quad (25)$$

## Gain factor

At  $T \neq 0$  the CNT conduction band is partially filled with electrons to Fermi level of  $E_{Fc}$ , and valence band — is empty up to Fermi level of  $E_{Fv}$ . Electrons from the conduction band pass into the valence band with photon emission in the energy range  $E_g < \hbar\omega < E_{Fc} - E_{Fv}$ , (where  $E_{Fv} < 0$ ), while the absorption coefficients (24) and (25)  $I = I_0 R_1 R_2 e^{2\alpha L}$  change sign from minus to plus [37]. In this case, an amplification of plasmon-polariton wave occurs, i.e., generation of a nanolaser. If the photon energy of the

external electromagnetic field (pumping) is  $\hbar\omega_p < E_g$ , then the absorption coefficient is  $\alpha_{\text{TM,TE}}(\omega) = 0$ , and absorption is  $\alpha_{\text{TM,TE}}(\omega) < 0$  occurs at the pumping photon energy of  $\hbar\omega_p > E_{Fc} - E_{Fv}$ . Thus, during pumping, an inversion of the energy state occurs in the system if the energy of the pumping photons stays within  $\hbar\omega_p > E_{Fc} - E_{Fv}$ , and photons with energy  $E_g < \hbar\omega < E_{Fc} - E_{Fv}$  are emitted by the inverted CNT medium.

The nanolaser should be pumped with optical radiation at a frequency at which the absorbed energy of the pumping photons will allow electrons to move from the valence band to the conduction band of „zigzag“ CNT into unoccupied energy levels. In this case, electrons from the conduction band pass into the valence band with photon emission at the laser transition frequency, which depends on the length of nanoresonator formed in CNT by Bragg gratings. Surface plasmons are excited in a plasmon laser nanoresonator as a result of hybridization of emitted photons at the laser transition frequency and electron oscillations in CNT conduction band, which leads to the generation of coherent plasmon waves.

The expressions for the gain factors (24) and (25) include the squares of the matrix elements of the dipole disturbance Hamiltonian for TM and TE modes that can be found through the relaxation frequency  $\Gamma = A_{mn}$  (Appendix C). Then, we get the nanolaser gain factor as

$$\alpha(\omega) = \frac{3c^2(2m_{vc})^{3/2}\Gamma \sqrt{\hbar\omega - E_g}}{2\sqrt{\beta_0^2/k_0^2 + \varepsilon} \hbar^2 \omega^2}, \quad (26)$$

where  $\beta_0$  — CNT's TM- or TE-mode propagation constant, respectively.

The change in the population of levels in CNT for the generation of coherent plasmon waves in the nanolaser during its pumping and radiation is also due to nonlinear effects of jcite35-37, which leads to saturation of the mode gain factors:

$$\alpha_{\text{TM}}, \alpha_{\text{TE}} \sim (1 + I_\omega/I_s)^{-1},$$

where  $I_\omega$  and  $I_s$  — the intensity of the plasmon flow at the generation frequency and the saturation intensity from the nanolaser amplification.

## Nanolaser parameters

Let's assume that nanolaser is generated at a telecommunication frequency of  $\omega = 2\pi c/\lambda_0 = 1.216 \cdot 10^{15} \text{ s}^{-1}$  ( $\lambda_0 = 1.55 \mu\text{m}$  in the air, 0.8 eV). We assume that the overlapping integral  $\gamma_{AB} = 2.7 \text{ eV}$  (in the dispersion equation (14)), and the number of electrons per „zigzag“ CNT unit volume  $N_e = 1.8 \cdot 10^{12} \text{ cm}^{-3}$  (in expression (20)). In this case, the dielectric permittivity of CNT at this frequency is  $\varepsilon_c \cong 1.0 + i1.0$ . At this concentration of electrons in the conduction band, relaxation frequency  $\Gamma = \frac{2e^6 \omega}{3\hbar^3 c^3} = 3.13 \cdot 10^8 \text{ s}^{-1}$ , CNT permittivity  $\varepsilon_c$ , and that

for the CNT surrounding medium  $\varepsilon = 2.09$  for the „zigzag“ CNT with indices (17.0) and radius  $r_0 = 0.665$  nm for modes with zero azimuthal indices from the equations (8) and (9) the following propagation constants can be found: TM-mode  $\beta_{0\text{TM}} = 5.62 \cdot 10^5 \text{ cm}^{-1}$  ( $\lambda_{\text{TM}} = 112$  nm) and TE-mode  $\beta_{0\text{TE}} = 4.51 \cdot 10^5 \text{ cm}^{-1}$  ( $\lambda_{\text{TE}} = 140$  nm).

„zigzag“ CNT with indices (17.0) has a radius  $r_0 = 0.665$  nm, inhomogeneities of CNT boundary representing the Bragg resonator gratings (Fig3) have a radius  $r_h = 0.509$  nm (CNT indices (13.0)). For the input mirror (left Bragg grating, Fig. 1) when repeating the CNT regions (13.0)  $n_1 = 4$  times and for the output mirror (right grating, Fig. 1) when repeating  $n_2 = 4$  times the reflection coefficients of the nanoresonator in terms of intensity will be calculated as  $R_1 = \rho_{(n_1)}\rho_{(n_1)}^*$  (input) and  $R_2 = \rho_{(n_2)}\rho_{(n_2)}^*$  (output) mirrors. The mode propagation constants for CNT inhomogeneities (13.0) have a value  $\beta_{0\text{TM}} = 6.27 \cdot 10^5 \text{ cm}^{-1}$  and  $\beta_{0\text{TE}} = 5.04 \cdot 10^5 \text{ cm}^{-1}$ , reflection coefficients  $R_{1\text{TM}} = R_{2\text{TM}} = 0.173$  and  $R_{1\text{TE}} = R_{2\text{TE}} = 0.175$ , Q-factor  $Q_{\text{TM}} = 10$  and  $Q_{\text{TE}} = 8$ , threshold generation coefficients (expression (13))  $\alpha_{0\text{TM}} = 1.76 \cdot 10^4 \text{ cm}^{-1}$  and  $\alpha_{0\text{TE}} = 1.74 \cdot 10^4 \text{ cm}^{-1}$ .

From the expression (16) for  $k_x = 0$ , we find the value of the band gap in „zigzag“ CNT equal to  $E_g = 0.586$  eV. For the electron wave vector  $k = 0.51 \cdot 10^7 \text{ cm}^{-1}$  in the forward interband transition at  $\omega = 1.216 \cdot 10^{15} \text{ s}^{-1}$  (0.8 eV) we find the reduced effective electron mass  $m_{vc} = m_v m_c / (m_v + m_c)$ . At the generation frequency, taking into account the symmetry of the spectral branches (Fig. 4), from expression (16) we find  $m_v = m_c = (d^2 \Delta E / d p_x^2)^{-1}$ , where  $p_x = \hbar k_x$ , and obtain the value of the reduced mass  $m_{vc} = m_c / 2 = 0.91 \cdot 10^{-28} \text{ g}$ .

Substituting the calculated parameters into (26), we find the values of the nanolaser gain factors for TM-mode  $\alpha_{\text{TM}} = 5.10 \cdot 10^4 \text{ cm}^{-1}$  and for TE-mode  $\alpha_{\text{TE}} = 6.34 \cdot 10^4 \text{ cm}^{-1}$ , which exceed the generation thresholds for the „zigzag“ CNT nanoresonator for the TM-mode by 2.9 times and for the TE-mode by 3.6 times.

For a nanoresonator of minimal length, given that Bragg gratings  $L_{\text{TM}} \cong 592$  nm (the volume of the mode field  $V_{\text{TM}} = 5.94 \cdot 10^5 \text{ nm}^3$ ), the Purcell coefficient  $F_{\text{TM}} = \frac{3\lambda_{\text{TM}}^3}{4\pi^2} \frac{Q}{V} = 1.79$  if generated at TM-mode. When the generation threshold for the intensity of the plasmon-polariton flux is exceeded, the CNT nanolaser generates coherent radiation in the TM mode with a frequency of  $\omega = 2\pi c / \lambda_0 = 1.216 \cdot 10^{15} \text{ s}^{-1}$  and a line width of  $\Delta\omega_r = F_{\text{TM}}\Gamma = 5.59 \cdot 10^8 \text{ s}^{-1}$ . When generated at TE-mode, the nanolaser has the following parameters:  $L_{\text{TE}} \cong 737$  nm ( $V_{\text{TE}} = 11.6 \cdot 10^5 \text{ nm}^3$ ),  $F_{\text{TE}} = 1.42$ ,  $\Delta\omega_r = 4.45 \cdot 10^8 \text{ s}^{-1}$ .

To pump a nanolaser generating at a telecommunication frequency (0.8 eV), a semiconductor quantum dot can be used, e.g., based on GaAs with a photon energy of 1.25–1.48 eV, i.e., the pumping photon energy should be higher than the level difference of the required laser transition 0.8 eV.

For a semiconductor quantum dot, as well as from CNT, a heat sink shall be deployed in a nanolaser to meet the condition for the number of activated interband transitions:

$$N_c / N_v = \exp[(E_c - E_v) / k_B T] > 1,$$

what follows from the Boltzmann formula, where  $k_B$  is the Boltzmann constant,  $T$  is the temperature of CNT during generation of plasmon waves in a nanolaser. For stable generation of coherent plasmon waves in a nanolaser, thermal stabilization of the system is required.

In the considered linear idealized model, the stationary generation mode is investigated in order to demonstrate the feasibility of a CNT nanolaser.

## Conclusion

Optical radiation pumping of a CNT nanoresonator with a „zigzag“ chirality and semiconductor properties increases the concentration of electrons in the conduction band. In these conditions the nanolaser may generate a flow of surface plasmon polaritons in a nanoresonator with Bragg gratings as periodic inhomogeneities at the ends of CNT. When the gain factor exceeds the threshold value, the CNT nanolaser generates a flow of coherent surface plasmon polaritons, which can be removed from the nanolaser to the CNT plasmon waveguide. The wavelength of coherent plasmon polaritons depends on the nanoresonator length, in particular, generation is possible at a telecommunication frequency corresponding to the wavelength in air 1.55  $\mu\text{m}$ .

## Acknowledgments

The authors express their gratitude to S.V. Tomilin for fruitful discussion of the findings.

## Funding

This study was supported by the Russian Science Foundation, grant № 19-72-20154, <https://rscf.ru/project/19-72-20154>.

## Conflict of interest

The authors declare no conflict of interest.

## Appendix A

By substituting into Leontovich boundary conditions  $E_z = \xi H_\varphi$  and  $H_z = E_\varphi / \xi$  [34] the expressions (1) for the modes components,

$$AK_l(w) = \xi \frac{r_0}{w^2} [Bl\beta K_l(w) - Aik_0 \varepsilon w K_l'(w)],$$

$$BK_l(w) = \frac{r_0}{\xi w^2} [Al\beta K_l(w) + Bik_0 w K_l'(w)],$$

we obtain a system of homogeneous linear equations for the amplitudes  $A$  and  $B$ :

$$\begin{aligned} \left[ K_l(w) + i\xi \frac{\varepsilon k_0 r_0}{w} K_l'(w) \right] A - \left[ \xi \frac{l\beta r_0}{w^2} K_l(w) \right] B &= 0, \\ \left[ \frac{l\beta r_0}{\xi w^2} K_l(w) \right] A + \left[ i \frac{k_0 r_0}{\xi w} K_l'(w) - K_l(w) \right] B &= 0 \end{aligned} \quad (\text{A1})$$

and find its determinant

$$\begin{aligned} D &= -K_l^2(w) - i\xi \frac{\varepsilon k_0 r_0}{w} K_l(w) K_l'(w) \\ &+ i \frac{k_0 r_0}{\xi w} K_l(w) K_l'(w) - \varepsilon \frac{k_0^2 r_0^2}{w^2} K_l'^2(w) + l^2 \frac{\beta^2 r_0^2}{w^4} K_l^2(w). \end{aligned} \quad (\text{A2})$$

Equating the determinants (A2) to zero, we obtain the equation

$$\begin{aligned} K_l^2(w) + \varepsilon \frac{k_0^2 r_0^2}{w^2} K_l'^2(w) + i \left( \xi \varepsilon - \frac{1}{\xi} \right) \\ \times \frac{k_0 r_0}{w} K_l(w) K_l'(w) = l^2 \frac{\beta^2 r_0^2}{w^4} K_l^2(w). \end{aligned} \quad (\text{A3})$$

Considering that for CNT with  $\mu_c = 1$  the impedance is  $\xi = 1/\sqrt{\varepsilon_c}$ , we find that the coefficient before the third term of equation (A3) is  $\xi \varepsilon - \frac{1}{\xi} = \frac{\varepsilon - \varepsilon_c}{\sqrt{\varepsilon_c}}$ . Then, from equation (A3), we obtain the dispersion equation for the propagation constants  $\beta_l(\omega)$  of plasmon-polariton CNT modes as

$$\begin{aligned} K_l^2(w) + \varepsilon \frac{k_0^2 r_0^2}{w^2} K_l'^2(w) + i \frac{\varepsilon - \varepsilon_c}{\sqrt{\varepsilon_c}} \\ \times \frac{k_0 r_0}{w} K_l(w) K_l'(w) = l^2 \frac{\beta^2 r_0^2}{w^4} K_l^2(w). \end{aligned} \quad (\text{A4})$$

For the modes with azimuthal index  $l = 0$  from the equation (A4) allowing for Macdonald function  $K_0'(w) = -K_1(w)$  we get a dispersion equation

$$K_0^2(w) + \varepsilon \frac{k_0^2 r_0^2}{w^2} K_1^2(w) - i \frac{\varepsilon - \varepsilon_c}{\sqrt{\varepsilon_c}} \frac{k_0 r_0}{w} K_0(w) K_1(w) = 0. \quad (\text{A5})$$

Representing equation (A5) in the form

$$\frac{K_1^2(w)}{K_0^2(w)} - i \frac{\varepsilon - \varepsilon_c}{\varepsilon \sqrt{\varepsilon_c}} \frac{w}{k_0 r_0} \frac{K_1(w)}{K_0(w)} + \frac{w^2}{\varepsilon k_0^2 r_0^2} = 0$$

and denoting  $K_1(w)K_0^{-1}(w) = \gamma$ , we look for the roots of the quadratic equation  $\gamma^2 - ia_1\gamma + a_2 = 0$ , where  $a_1 = \frac{\varepsilon - \varepsilon_c}{\varepsilon \sqrt{\varepsilon_c}} \frac{w}{k_0 r_0}$ ,  $a_2 = \frac{w^2}{\varepsilon k_0^2 r_0^2}$ ; we get

$$\gamma_{1,2} = i \left( \frac{a_1}{2} \pm \sqrt{\frac{a_1^2}{4} + a_2} \right). \text{ From here we find that}$$

$$\gamma_{1,2} = i \frac{w}{k_0 r_0} \left( \frac{\varepsilon - \varepsilon_c}{2\varepsilon \sqrt{\varepsilon_c}} \pm \sqrt{\frac{(\varepsilon - \varepsilon_c)^2}{4\varepsilon^2 \varepsilon_c} + \frac{1}{\varepsilon}} \right),$$

i.e. roots of the equation are as follows

$$\gamma_1 = i \frac{w}{\sqrt{\varepsilon_c} k_0 r_0}, \quad \gamma_2 = -i \frac{w \sqrt{\varepsilon_c}}{\varepsilon k_0 r_0}.$$

## Appendix B

The continuity conditions for the tangential components of the nanoresonator mode incident on the inhomogeneity in the resonator (i — incident, r — reflected, t — transmitted) are expressed as [39] for TM-mode

$$E_{ri} + E_{rr} = E_{rt}, \quad H_{\phi i} - H_{\phi r} = H_{\phi t}$$

and for TE-mode

$$H_{ri} + H_{rr} = H_{rt}, \quad E_{\phi i} - E_{\phi r} = E_{\phi t}.$$

From expressions (6) and (7) we find the connection of the components of TM-mode:  $H_\phi = \frac{\varepsilon k_0}{\beta_0} E_r$  and TE-mode:  $H_r = -\frac{\beta_0}{k_0} E_\phi$ . The continuity conditions for the forward (+) and backward (−) modes inside the inhomogeneity have the form  $E = E^+ + E^-$ ,  $H = H^+ + H^-$ . Then we obtain the relations for the TM-mode  $E_h = E_{ri} + E_{rr}$ ,  $H_h = \frac{\varepsilon k_0}{\beta_{0h}} (E_{ri} - E_{rr})$  and for the TE-mode  $H_h = (-\frac{\beta_0}{k_0})(E_{\phi i} + E_{\phi r})$ ,  $E_h = E_{\phi i} - E_{\phi r}$ . These expressions have the following form: for TM mode

$$E_h = Ae^{i\beta_{0h}y} + Be^{-i\beta_{0h}y}, \quad H_h = \frac{\varepsilon k_0}{\beta_{0h}} (Ae^{i\beta_{0h}y} - Be^{-i\beta_{0h}y}) \quad (\text{B1})$$

and for TE-mode

$$E_h = Ae^{i\beta_{0h}y} - Be^{-i\beta_{0h}y}, \quad H_h = \left( -\frac{\beta_0}{k_0} \right) (Ae^{i\beta_{0h}y} + Be^{-i\beta_{0h}y}). \quad (\text{B2})$$

Given the continuity of the tangential components of the modes on the left  $y = 0$  and right  $y = d$  boundaries of one inhomogeneity in the CNT, we obtain systems of equations from expressions (B1) and (B2). Excluding the amplitudes  $A$  and  $B$  from the obtained equations, we find unimodular matrices for the TM-mode

$$\begin{aligned} \begin{pmatrix} E_0 \\ H_0 \end{pmatrix} &= \begin{pmatrix} \cos(\beta_{0h}d) & -i \frac{\beta_{0h}}{\varepsilon k_0} \sin(\beta_{0h}d) \\ -i \frac{\varepsilon k_0}{\beta_{0h}} \sin(\beta_{0h}d) & \cos(\beta_{0h}d) \end{pmatrix} \begin{pmatrix} E_d \\ H_d \end{pmatrix} \\ &= M_{\text{TM1}} \begin{pmatrix} E_d \\ H_d \end{pmatrix} \end{aligned} \quad (\text{B3})$$

and for TE-mode

$$\begin{aligned} \begin{pmatrix} E_0 \\ H_0 \end{pmatrix} &= \begin{pmatrix} \cos(\beta_{0h}d) & i \frac{k_0}{\beta_0} \sin(\beta_{0h}d) \\ i \frac{\beta_0}{k_0} \sin(\beta_{0h}d) & \cos(\beta_{0h}d) \end{pmatrix} \begin{pmatrix} E_d \\ H_d \end{pmatrix} \\ &= M_{\text{TE1}} \begin{pmatrix} E_d \\ H_d \end{pmatrix}. \end{aligned} \quad (\text{B4})$$

For  $N$  inhomogeneities with a width  $d_j$  along the coordinate  $y = d_1 + d_2 + \dots + d_N$  we get in the last plane  $N + 1$  the expression

$$\begin{pmatrix} E_0 \\ H_0 \end{pmatrix} = M_1 M_2 \dots M_N \begin{pmatrix} E_{N+1} \\ H_{N+1} \end{pmatrix}. \quad (\text{B5})$$

The product of  $N$  unimodular matrices characterizes the Bragg grating

$$M = \begin{pmatrix} m_{11} & m_{12} \\ m_{21} & m_{22} \end{pmatrix} = \prod_{j=1}^N M_j. \quad (\text{B6})$$

The elements  $m_{ij}$  of the matrix  $M$  are found using expressions for the unimodular matrix for the TM mode (B3) and the matrix for the TE mode (B4); we obtain the equations for the TM-mode

$$\begin{aligned} E_{ri} + E_{rr} &= \left( m_{11} + m_{12} \frac{\epsilon k_0}{\beta_0} \right) E_{rt}, \\ E_{ri} - E_{rr} &= \left( \frac{\beta_0}{\epsilon k_0} m_{21} + m_{22} \right) E_{rt} \end{aligned} \quad (\text{B7})$$

and for TE-mode

$$\begin{aligned} E_{\phi i} - E_{\phi r} &= \left( m_{11} - \frac{\beta_0}{k_0} m_{12} \right) E_{\phi t}, \\ E_{\phi i} + E_{\phi r} &= \left( m_{22} - \frac{k_0}{\beta_0} m_{21} \right) E_{\phi t}. \end{aligned} \quad (\text{B8})$$

From equations (B7) and (B8) we find the amplitude coefficients of transmission  $\tau$  and reflection  $\rho$  for TM mode

$$\begin{aligned} \tau &= \frac{E_{rt}}{E_{ri}} = \frac{2}{m_{11} + m_{12} \frac{\epsilon k_0}{\beta_0} + \frac{\beta_0}{\epsilon k_0} m_{21} + m_{22}}, \\ \rho &= \frac{E_{rr}}{E_{ri}} = \frac{m_{11} + m_{12} \frac{\epsilon k_0}{\beta_0} - \frac{\beta_0}{\epsilon k_0} m_{21} - m_{22}}{m_{11} + m_{12} \frac{\epsilon k_0}{\beta_0} + \frac{\beta_0}{\epsilon k_0} m_{21} + m_{22}} \end{aligned} \quad (\text{B9})$$

and for TE-mode

$$\begin{aligned} \tau &= \frac{E_{\phi t}}{E_{\phi i}} = \frac{2}{m_{11} - \frac{\beta_0}{k_0} m_{12} - \frac{k_0}{\beta_0} m_{21} + m_{22}}, \\ \rho &= \frac{E_{\phi r}}{E_{\phi i}} = \frac{m_{22} - \frac{k_0}{\beta_0} m_{21} - m_{11} + \frac{\beta_0}{k_0} m_{12}}{m_{11} - \frac{\beta_0}{k_0} m_{12} - \frac{k_0}{\beta_0} m_{21} + m_{22}}. \end{aligned} \quad (\text{B10})$$

## Appendix C

The average dipole moment  $\langle \mathbf{d}_1 \rangle$  of an electron, taking into account the relaxation frequencies (spontaneous emission) for electronic transitions, is [38]

$$\langle \mathbf{d}_1 \rangle = \frac{e^2 \mathbf{E}_a}{2\hbar} \sum_n |r_{n0}|^2 \left( \frac{e^{i\omega t}}{\omega_{n0} - i\Gamma_n/2 + \omega} + \frac{e^{-i\omega t}}{\omega_{n0} - i\Gamma_n/2 - \omega} + \frac{e^{i\omega t}}{\omega_{n0} - i\Gamma_n/2 - \omega} + \frac{e^{-i\omega t}}{\omega_{n0} - i\Gamma_n/2 + \omega} \right), \quad (\text{C1})$$

from where we find

$$\begin{aligned} \langle \mathbf{d}_1 \rangle &= \frac{e^2 \mathbf{E}_a \cos(\omega t)}{\hbar} \sum_n |r_{n0}|^2 \\ &\times \left( \frac{1}{\omega_{n0} - i\Gamma_n/2 + \omega} + \frac{1}{\omega_{n0} - i\Gamma_n/2 - \omega} \right). \end{aligned} \quad (\text{C2})$$

Converting the expression (C2), we obtain the dipole moment of the electron, providing for resonant absorption and spontaneous emission in CNT, in the form

$$\langle \mathbf{d}_1 \rangle = \frac{2e^2 \mathbf{E}_a \cos(\omega t)}{\hbar} \sum_n |r_{n0}|^2 \frac{\omega_{n0} - i\Gamma_n/2}{(\omega_{n0} - i\Gamma_n/2)^2 - \omega^2}. \quad (\text{C3})$$

The dielectric permittivity of C is found using the expression for the induction vector  $\mathbf{D} = \mathbf{E} + 4\pi\mathbf{P} = \epsilon\mathbf{E}$  substituting the average dipole electron moment (C2) into the polarization vector of the medium  $\mathbf{P} = \langle \mathbf{d}_1 \rangle N_e$ , where  $N_e$  is the number of electrons per unit volume,

$$\epsilon_c(\omega) = 1 + \frac{2m\omega_e^2}{\hbar} \sum_n |r_{n0}|^2 \frac{\omega_{n0} - i\Gamma_n/2}{(\omega_{n0} - i\Gamma_n/2)^2 - \omega^2}. \quad (\text{C4})$$

Here  $\omega_e^2 = 4\pi e^2 N_e / m$  — the electron plasma frequency,  $m$  — the effective mass of the electron.

We assume that plasmon-polariton modes are excited at the frequency of the direct electron transition  $\omega = \omega_{nm'}$  in CNT. Then the electron dipole moment (C2) is

$$\langle \mathbf{d}_1 \rangle = \frac{2E_a \cos(\omega t) e^2 |r_{nm'}|^2}{\hbar} \left( \frac{1}{4\omega - i\Gamma} + \frac{i}{\Gamma} \right). \quad (\text{C5})$$

Substituting the dipole electronic moment (C5) into the polarization vector of the medium, we obtain the expression for the CNT dielectric permittivity during photon emission (absorption) at the electronic transition frequency  $\omega$ ,

$$\begin{aligned} \epsilon_c(\omega) &= 1 + \frac{8\pi e^2 |r_{nm'}|^2 N_e}{\hbar} \left[ \frac{4\omega}{16\omega^2 + \Gamma^2} \right. \\ &\quad \left. + \frac{i}{\Gamma} \left( 1 + \frac{\Gamma^2}{16\omega^2 + \Gamma^2} \right) \right]. \end{aligned} \quad (\text{C6})$$

Let's find the relaxation frequency  $\Gamma_n$  as the inverse of the lifetime of the electron  $\tau_n = 1/A_{n0}$  in the conduction band before the forward transition to the valence band. The energy density emitted by an electron during a dipole transition per unit time is determined by integrating the Poynting vector with modulus

$$S = \frac{c}{4\pi} \frac{(d^r)^2}{r^2} \frac{\omega^4}{c^4} \sin^2 \theta$$

at  $\omega r/c \ll 1$  over a surface with radius  $r = a$ , surrounding the dipole,  $d^r = -er_{n0} \exp(-i\omega t) + \text{c.c.}$  [40]. Given the values of the time average square of the dipole moment

$$\overline{(d^r)^2} = \overline{(2d_0^r \cos \omega t)^2} = 2(d_0^r)^2$$

and integral over the surface

$$r^2 \int_0^{2\pi} d\varphi \int_0^\pi S \sin \theta d\theta = \frac{4\pi r^2}{3} \frac{c}{4\pi} \frac{(d^r)^2}{r^2} \frac{\omega^4}{c^4}$$

we find the energy density of the dipole radiation per unit time

$$E_1 = \frac{2e^2 \omega_{n0}^4}{3c^3} (r_{n0})^2.$$

The Einstein coefficient [37.40] for spontaneous oscillator radiation  $A_{n0}$  is equal to the oscillator radiation energy per unit time divided by the photon energy  $\hbar\omega_{n0}$ , i.e., the relaxation frequency is

$$\Gamma_n = A_{n0} = \frac{2e^2\omega_{n0}^3}{3\hbar c^3} |r_{n0}|^2.$$

Assuming that the ratio  $e^2/r_{n0} = \hbar\omega_{n0}$  holds for an electron during a direct transition from the conduction band to the valence band, we find the relaxation frequency  $\Gamma_n = \frac{2e^6\omega_{n0}}{3\hbar^2 c^3}$ .

## Appendix D

Poynting vector of TM-mode ( $E_r, H_\phi, E_z$ ) is equal

$$\mathbf{S} = \frac{c}{4\pi} [\mathbf{1}_r(-E_z H_\phi) + \mathbf{1}_z(E_r H_\phi)].$$

For the real values of the mode components, the time-averaged Poynting vector is

$$\bar{\mathbf{S}} = \frac{c}{8\pi} [-\mathbf{1}_r(E_z H_\phi^* + H_\phi E_z^*) + \mathbf{1}_z(E_r H_\phi^* + H_\phi E_r^*)].$$

On the CNT surface at  $r = r_0$ , we find the modulus of the Poynting vector for the TM-mode

$$\begin{aligned} \bar{S}_{\text{TM}} &= \frac{c}{8\pi} [(E_z H_\phi^* + H_\phi E_z^*)^2 + (E_r H_\phi^* + H_\phi E_r^*)^2]^{1/2} \\ &= \frac{c}{4\pi} S_{\text{TM}} A^2, \end{aligned}$$

where  $S_{\text{TM}} = \sqrt{\beta_0^2/k_0^2 + \varepsilon}$ .

Poynting vector of TE-mode ( $H_r, E_\phi, H_z$ ) is equal

$$\mathbf{S} = \frac{c}{4\pi} [\mathbf{1}_r(E_\phi H_z) + \mathbf{1}_z(-E_\phi H_r)],$$

and by averaging in time we get

$$\bar{\mathbf{S}} = \frac{c}{8\pi} [\mathbf{1}_r(E_\phi H_z^* + H_z E_\phi^*) - \mathbf{1}_z(E_\phi H_r^* + H_r E_\phi^*)],$$

i. e.

$$\begin{aligned} \bar{S}_{\text{TE}} &= \frac{c}{8\pi} [(E_\phi H_z^* + H_z E_\phi^*)^2 + (E_\phi H_r^* + H_r E_\phi^*)^2]^{1/2} \\ &= \frac{c}{4\pi} S_{\text{TE}} B^2, \end{aligned}$$

where  $S_{\text{TE}} = \varepsilon^{-1} \sqrt{\beta_0^2/k_0^2 + \varepsilon}$ .

Matrix element of the disturbance Hamiltonian on the CNT surface at  $r = r_0$  for TM-mode

$$\hat{H}'_{vc} = \frac{eA}{2} \int dz \psi_v^*(y) z \psi_c(y) = \frac{eE_z}{2} y_{vc},$$

for TE-mode

$$\hat{H}'_{vc} = \frac{er_0 B}{2} \int d\phi \psi_v^*(\phi) \phi \psi_c(\phi) = \frac{er_0 E_\phi}{2} \phi_{vc},$$

squares of matrix elements for TM-mode

$$|\hat{H}'_{vc}|^2 = \frac{e^2 E_z^2}{4} |y_{vc}|^2 = \frac{e^2 A^2}{4} |y_{vc}|^2,$$

for TE-mode

$$|\hat{H}'_{vc}|^2 = \frac{e^2 r_0^2 E_\phi^2}{4} |\phi_{vc}|^2 = \frac{e^2 r_0^2 B^2}{4} |\phi_{vc}|^2.$$

## References

- [1] M.I. Stockman. *Opt. Express*, **19** (22), 22029 (2011).
- [2] A.P. Vinogradov, E.S. Andrianov, A.A. Pukhov, A.V. Dorofeenko, A.A. Lisysansky. *UFN*, **182** (10), 1122 (2012) (in Russian). DOI: 10.3367/UFNr.0182.201210j.1122
- [3] V.I. Balykin. *UFN*, **188** (9), 935 (2018) (in Russian). DOI: 10.3367/UFNr.2017.09.038206
- [4] V.V. Klimov. *UFN*, **193** (3), 279 (2023) (in Russian). DOI: 10.3367/UFNr.2022.02.039153
- [5] M.Yu. Gubin, A.Yu. Leksin, A.V. Shesterikov, A.V. Prokhorov, V.S. Volkov. *Nanomaterials*, **10**, 122 (2020). DOI: 10.3390/nano10010122
- [6] M.Yu. Gubin, I.V. Dzedolik, T.V. Prokhorova, V.S. Pereskokov, A.Yu. Lexin. *Opt. i spektr.*, **130** (3), 448 (2022) (in Russian). DOI: 10.21883/OS.2022.03.52176.2700-21
- [7] I.V. Dzedolik, S.V. Tomilin, S.N. Polulyakh, B.M. Yakubenko. *St. Petersburg State Polytech. Univ. J. Phys. Math.*, **16** (3.1), 163 (2023). DOI: 10.18721/JPM.163.129
- [8] S.I. Azzam, A.V. Kildishev, R.-M. Ma, C.-Z. Ning, R. Oulton, V.M. Shalaev, M.I. Stockman, J.-L. Xu, X. Zhang. *Light: Sci. Appl.*, **9**, 90 (2020). DOI: 10.1038/s41377-020-0319-7
- [9] M.Yu. Gubin, A.V. Shesterikov, S.N. Karpov, A.V. Prokhorov. *Phys. Rev. B*, **97**, 085431 (2018). DOI: 10.1103/PhysRevB.97.085431
- [10] R.-M. Ma, S.-Y. Wang. *Nanophotonics*, **0298** (2021). DOI: 10.1515/nanoph-2021-0298
- [11] D.J. Bergman, M.I. Stockman. *Phys. Rev. Lett.*, **90** (2), 027402 (2003). DOI: 10.1103/PhysRevLett.90.027402
- [12] I.E. Protsenko. *UFN*, **182** (10), 1116 (2012) (in Russian). DOI: 10.3367/UFNr.0182.201210i.1116
- [13] M.A. Noginov, G. Zhu, A.M. Belgrave, R. Bakker, V.M. Shalaev, E.E. Narimanov, S. Stout, E. Herz, T. Suteewong, U. Wiesner. *Nature*, **460**, 1110 (2009). DOI: 10.1038/nature08318
- [14] M.I. Stockman. *Adv. Photon.*, **2** (5), 054002 (2020). DOI: 10.1117/1.AP.2.5.054002
- [15] C. Jayasekara, M. Premaratne, M.I. Stockman, S.D. Gunapala. *J. Appl. Phys.*, **118**, 173101 (2015).
- [16] I.O. Zolotovskii, Yu.S. Dadoenkova, S.G. Moiseev, A.S. Kadochkin, V.V. Svetukhin, A.A. Fotiadi. *Phys. Rev. A*, **97**, 053828 (2018). DOI: 10.1103/PhysRevA.97.053828
- [17] H. Li, Z.-T. Huang, K.-B. Hong, M.-W. Yu, C.-H. Wu, C.-S. Yang, T.-R. Lin, K.-P. Chen, T.-C. Lu. *J. Appl. Phys.*, **131**, 011101 (2022). DOI: 10.1063/5.0061329
- [18] J. Wang, W. Wei, X. Yan, J. Zhang, X. Zhang, X. Ren. *Opt. Express*, **25** (8), 9358 (2017). DOI: 10.1364/OE.25.009358
- [19] M.J.H. Marell, B. Smalbrugge, E.J. Geluk, P.J. van Veldhoven, B. Barcones, B. Koopmans, R. Nötzel, M.K. Smit, M.T. Hill. *Opt. Express*, **19** (16), 15109 (2011).

- [20] C. Couteau, A. Larrue, C. Wilhelm, C. Soci. *Nanophotonics*, **4**, 90 (2015). DOI: 10.1515/nanoph-2015-0005
- [21] L. Xu, F. Li, Y. Liu, F. Yao, S. Liu. *Appl. Sci.*, **9**, 861 (2019). DOI: 10.3390/app9050861
- [22] Z. Gu, Q. Song, S. Xiao. *Front. Chemistry*, **8**, 613504 (2021). DOI: 10.3389/fchem.2020.613504
- [23] M.-S. Hwang, H.-R. Kim, K.-Y. Jeong, H.-G. Park, Yu. Kivshar. *Nanophotonics*, 0265 (2021). DOI: 10.1515/nanoph-2021-0265
- [24] O.V. Kibis, M.E. Portnoy. *Pisma v ZhTF* **31**(15), 85 (in Russian). (2005).
- [25] S. Iijima. *Lett. Nature*, **354**(11), 56 (1991).
- [26] R. Saito, M. Fujita, G. Dresselhaus, M.S. Dresselhaus. *Appl. Phys. Lett.*, **60**(18), 2204 (1992). DOI: 10.1063/1.107080
- [27] Yu.I. Lozovik, A.M. Popov. *UFN*, **167**(7), 751 (1997) (in Russian).
- [28] T. Ando. *J. Phys. Soc. Japan*, **74**(3), 777 (2005). DOI: 10.1143/JPSJ.74.777
- [29] M.B. Belonenko, N.G. Lebedev, E.V. Sochneva. *FTT* **53**(1), (in Russian). 194 (2011).
- [30] I.V. Dzedolik, A.D. Lyashko. *Opt. i Spekr.*, **132**(10), 1087 (2024). DOI: 10.61011/OS.2024.10.59424.5988-24
- [31] I.A. Aleksandrov, D.V. Chubukov, N.N. Rozanov. *Opt. i spektr.*, **131**(11), 1582 (2023) (in Russian). DOI: 10.61011/OS.2023.11.57029.129-23
- [32] N.N. Rozanov. *Opt. i spektr.*, **132**(8), 839 (2024) (in Russian). DOI: 10.61011/OS.2024.08.59030.136-24
- [33] P. Harris. *Carbon Nanotubes and Related Structures* (Tekhnosfera, M., 2003).
- [34] L.D. Landau, E.M. Lifshitz. *Electrodynamics of Continuous Media* (Nauka, Fiz.-mat.lit, 1982).
- [35] N.V. Karlov. *Lektsii po kvantovoy elektronike* (Nauka, Fiz.-mat. lit., M., 1988).
- [36] R. Pantel, G. Puthof. *Osnovy Kvantovoy Elektroniki* (Mir, M., 1972) (in Russian).
- [37] A. Yariv. *Kvantovaya elektronika i nelineynaya optika* (Sov. radio, M., 1973) (in Russian).
- [38] A.S. Davydov. *Kvantovaya mekhanika* (Fiz.-mat. lit., M., 1963) (in Russian).
- [39] M. Rousseau, J.P. Mathieu. *Zadachi po optike* (Mir, M., 1976) (in Russian).
- [40] R. Ditchbern. *Fizicheskaya optika* (Fiz.-mat.lit, M., 1965) (in Russian).

*Translated by T.Zorina*